### Title
Genetically encoded tools for measuring and manipulating metabolism




### Journal
Nature Chemical Biology, 18(5)

### ISSN
1552-4450



### Authors
Choe, Mangyu
Titov, Denis V



### Publication Date
2022-05-01

### DOI
10.1038/s41589-022-01012-8

Peer reviewed

HHS Public Access

Author manuscript

*Nat Chem Biol*. Author manuscript; available in PMC 2022 November 01.

Published in final edited form as:

*Nat Chem Biol*. 2022 May ; 18(5): 451–460. doi:10.1038/s41589-022-01012-8.

# Genetically encoded tools for measuring and manipulating metabolism

**Mangyu Choe**[1,2,3], **Denis V. Titov**[1,2,3,*]

[1]Department of Nutritional Sciences & Toxicology, University of California, Berkeley, CA, USA

[2]Center for Computational Biology, University of California, Berkeley, CA, USA

[3]Department of Molecular & Cell Biology, University of California, Berkeley, CA, USA

## Abstract

Over the last few years, we have seen an explosion of novel genetically encoded tools for measuring and manipulating metabolism in live cells and animals. Here we will review the genetically encoded tools that are available, describe how these tools can be used, and outline areas where future development is needed in this fast-paced field. We will focus on tools for direct measurement and manipulation of metabolites. Metabolites are master regulators of metabolism and physiology through their action on metabolic enzymes, signaling enzymes, ion channels, and transcription factors among others. We hope that this perspective will encourage more people to use these novel reagents or even join this exciting new field to develop novel tools for measuring and manipulating metabolism.

## Editorial summary:

This perspective discusses the genetically encoded tools for measuring and manipulating metabolism, highlighting the tools that are available, guidelines for their use, and key areas for future development.

## Graphical Abstract

[*]**Corresponding author statement:** titov@berkeley.edu.

**Conflict of Interest Statement:** D.V.T. is listed as an inventor on a patent application (US Patent App. 15/749,218) describing the use of LbNOX and TPNOX that are discussed in this perspective.

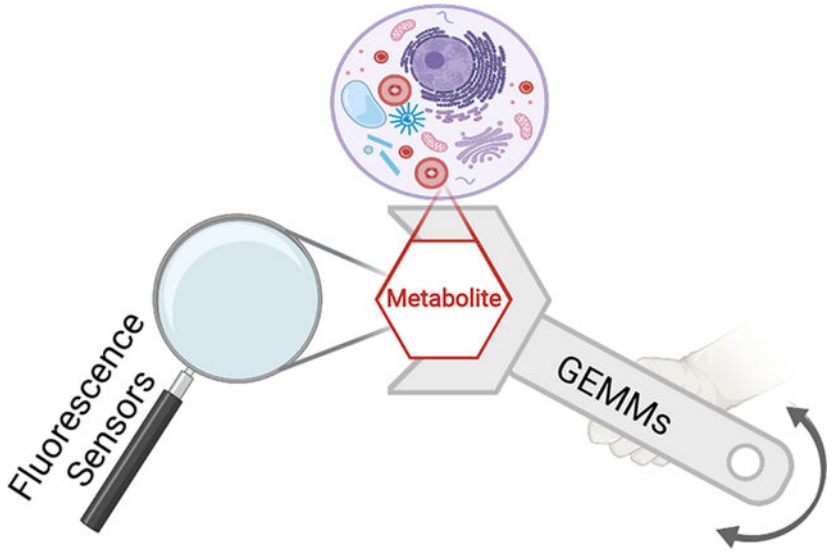


## Introduction

Albert Szent-Györgyi once said that “life is nothing but an electron looking for a place to rest”. Over the last century, the field of metabolism has made tremendous progress in the understanding of the metabolic pathways that fuel life. We have discovered and characterized most of the reactions and metabolic intermediates that make up pathways that produce energy and building blocks. We have a detailed understanding of reaction mechanisms catalyzed by metabolic enzymes and have atomic resolution structures for many of the enzymes. The next frontier in metabolism research is to quantitatively understand how these intricate pathways are regulated to match supply and demand for energy and building blocks and how changes in metabolism affect organismal phenotypes. There is a tremendous number of fascinating observations awaiting to be explained that connect metabolism to phenotypes including lifespan extension by calorie restriction[1], Warburg effect in cancer cells[2,3] and a seemingly endless list of beneficial effects of diet and exercise on age-associated diseases[4–7]. To unravel the mysteries of metabolic regulation, we need a new generation of tools for measuring and manipulating metabolism.

Metabolism is regulated by small molecules that directly modulate the activity of metabolic enzymes, signaling pathways, gene expression, and hormone levels (Figure 1). Metabolite levels are master regulators of metabolism and physiology through their direct effects on metabolic enzymes[8], kinases[9,10], transcription factors[11], ion channels[12] and hormone levels[12] among others. For example, biosynthetic pathways are regulated by the concentration of their end products such as amino acids, lipids, nucleotides, and cofactors[13]. Similarly, energy metabolism pathways are regulated by their end products such as ATP/ADP, NADH/$NAD^+$, NADPH/$NADP^+$, GSH/GSSH, Acetyl-CoA/CoA, $H_2O_2$, and mitochondrial membrane potential ($\Delta\Psi_m$)[13]. We want to highlight the often-discounted insight that products of energy metabolism are in fact ratios (referred to as bioenergetic ratios, henceforth). For example, ATP can drive unfavorable reactions inside the cells because the intracellular ATP/ADP ratio is maintained at a level ~$10^9$ higher than the

equilibrium value for ATP hydrolysis reaction. If ATP/ADP ratio was at equilibrium, then ATP would not be able to drive energy demanding processes regardless of its concentration. As a result of the latter, many metabolic enzymes, kinases, and ion channels evolved to be regulated by ATP/ADP ratio and not simply by ATP levels.

Metabolism is compartmentalized in subcellular organelles and tissues. For example, fatty acid biosynthesis occurs in the cytosol while β-oxidation of fatty acids takes place in the mitochondria. Similarly, liver can produce glucose through gluconeogenesis while most other tissues can only consume glucose. This compartmentalization is necessary because some metabolic pathways cannot operate under the same conditions or might produce futile cycles if allowed to occur in the same compartment. To facilitate compartment- and tissue-specific regulation of metabolism, organisms have evolved paralogous genes that code for enzymes that have different kinetic properties and are expressed in specific tissues (e.g., PFKP, PFKM, PFKL) or specific subcellular compartments (e.g., MDH1 and MDH2).

To better understand the regulation of metabolism, we need a new generation of tools to measure and manipulate the levels of individual metabolites and bioenergetic ratios in compartment- and tissue-specific manner. This approach will be complimentary to genetic and biochemical approaches of manipulating one enzyme or one pathway at a time and will allow researchers to investigate the systemic effects of pleiotropic regulators like ATP/ADP ratio that directly modulate dozens of metabolic enzymes, kinases, and ion channels. Compartment- and tissue-specific manipulation and measurement of metabolism is difficult to achieve using small molecule drugs to manipulate metabolism or bulk cell and tissue lysis to measure metabolism. Here, we will review genetically encoded tools that can be used to measure and manipulate metabolism in compartment- and tissue-specific manner by targeting them to subcellular compartments like mitochondria, nucleus, ER, lysosome, and by using tissues specific promoters. We will review some of the recent developments in this new field and highlight areas for future development. We are only beginning to scratch the surface in terms of our ability to measure and especially manipulate metabolism in tissue- and compartment-specific manner and we hope that this perspective will encourage more people to work in this area.

## Genetically encoded sensors for measuring metabolism

In this section, we will review the currently available genetically encoded fluorescence sensors for measuring metabolite levels and bioenergetic ratios. We will focus on protein-based genetically encoded fluorescence sensors that directly bind metabolites and can be used for real-time measurement of the compartment- and tissue-specific levels of metabolites. Several other types of sensors have been developed including small molecule probes[14], RNA-based biosensors[15], and transcription-based reporters[16]. We chose not to focus on the latter categories of excellent sensors primarily due to space constraints and because it can be more difficult to use these sensors for compartment-specific measurements as they cannot be easily targeted to subcellular compartments.

Genetically-encoded fluorescence sensors have been pioneered in the early 1990s and are now routinely used for studying cell signaling[17]. The basic fluorescence sensor consists of

two parts: a fluorescence protein(s) and a sensing domain (Figure 2). When a molecule binds to the sensing domain it changes the conformation of the sensor leading to a change in the fluorescence properties of the sensor. The change in the fluorescence properties of the sensor can be quantified using a fluorescence microscope or a fluorescence plate reader. Fluorescence properties that are most frequently measured include brightness (i.e., the product of quantum yield and extinction coefficient) and fluorescence lifetime at a particular excitation/emission (ex/em) wavelength pair. Fluorescence measurements can be further subdivided into single-channel and dual-channel (or ratiometric) measurements where one or two ex/em wavelength pairs are monitored, respectively. The dual-channel category includes Förster Resonance Energy Transfer (FRET) that is frequently used in fluorescence sensors.

Fluorescence sensors provide three unique insights about metabolite levels and bioenergetic ratios compared to bulk cell and tissue lysis methods. First, fluorescence sensors can be targeted to different subcellular compartments like mitochondria, nucleus, ER or lysosome to measure compartment-specific changes in metabolite levels and bioenergetic ratios. Second, fluorescence sensors measure the free metabolites levels and bioenergetic ratios while cell lysis methods measure the sum of free and protein-bound levels of metabolites. The latter is important because metabolites inside the cell exist as a mixture of free and protein-bound molecules, but only free metabolites are “visible” and can modulate the activity of proteins. Third, fluorescence sensors can be used to measure rapid changes in metabolite levels (i.e., with a time resolution of seconds for some sensors) that is difficult to achieve using bulk cell lysis approaches.

The key parameters that determine the functionality of the fluorescence sensor are its $EC_{50}$ (half maximal effective concentration) for sensed metabolite (or bioenergetic ratio), the specificity for sensed molecule(s), the dynamic range of fluorescence response (i.e., the difference between minimal and maximal signal divided by minimal signal ($\Delta F/F_{min}$)), the kinetics of fluorescence response, and brightness. It is important for the $EC_{50}$ for sensed molecule (or bioenergetic ratio) to be similar to the physiologically relevant concentrations of a sensed metabolite (or bioenergetic ratio) in order for the sensor to be useful for measurements in live cells. Similarly, the sensor must be specific for the sensed molecule, and it should not respond to changes in other molecules. Finally, a higher dynamic range of the sensor will allow researchers to detect smaller changes of the sensed molecule or ratio and high brightness and faster kinetics will simplify measurements.

Several fluorescence sensors for metabolites and bioenergetic ratios have been developed over the last two decades. Table 1 summarizes the key characteristics of select sensors including the range of sensed parameters that they can detect, a dynamic range of the sensor, values of sensed parameters that are observed in cells, and recommended positive control treatments that can be used to ensure that sensor is working. We hope that this summary together with the next section on the guidelines for using the sensors will be used as a starting reference point by investigators as they decide on the most appropriate sensor for specific applications. New sensors are regularly being reported and we did not have the space to include every available sensor so we encourage the readers to check the latest literature and databases like Fluorescent Biosensor Database[17] for more comprehensive and up-to-date information about the available sensors for their metabolites of interest.

Researchers have used several strategies to design fluorescence sensors for metabolites. The most common approach is to fuse a fluorescence protein with a naturally occurring domain that can sense a metabolite or bioenergetic ratio of interest. Amino acids included in the sensing domain and the sequence of linkers connecting the sensing domain and fluorescence protein are critical to achieving fluorescence response. Many combinations have to be tested before the design has any activity. Most sensors have been developed using this broad strategy. GSH/GSSG sensor GRX1-roGFP2[18] and $H_2O_2$ sensor Orp1-roGFP2[19,20] use a different approach where GRX1 and Orp1 are enzymes that use the GSH/GSSG or $H_2O_2$ as substrates to catalyze the change in redox state of the disulphide bond on roGFP2. Disulphide bond status of roGFP2 is then translated into change in fluorescence. Yet another approach is to use mutagenesis to switch the specificity of the sensor between closely related metabolites. The latter approach was used to engineer NADPH/$NADP^+$ sensor iNap[21] based on NADH/$NAD^+$ sensor SoNar[22].

## Guidelines for using genetically encoded sensors

Here we describe aspects of experimental design that should be considered when performing experiments with fluorescence sensors or choosing the best fluorescence sensor for specific applications. We discuss sensor calibration, normalization between experiments, and issues that might cause misinterpretation of the results such as a signal that is saturated or below the detection limit, slow response kinetics, pH sensitivity, and photobleaching misinterpreted as a signal. Many of these caveats can be managed using the approaches described below. The goal of this section is to discuss several points that are specifically related to the use of fluorescence sensors for measuring metabolites and bioenergetic ratios and we refer the reader to the many excellent reviews and books for more general info about fluorescence microscopy[23].

It is important to establish that the fluorescence sensor can respond to changes in sensed metabolite or bioenergetic ratio under specific experimental conditions. For example, the sensor will not report any change in fluorescence even when the sensed parameter is changing if it is saturated or if its response kinetics are not fast enough to observe a change within a time frame of an experiment. One way to confirm that the fluorescence sensor is working under specific conditions is to increase or decrease the sensed parameter and confirm that the fluorescence sensor signal changes accordingly in response. Suggestions for control treatments for available sensors are provided in Table 1. Sensors with various $EC_{50}$ and response kinetics are available for many metabolites and bioenergetic ratios so several sensors can be tried to find the version that is not saturated or below the detection limit and has a fast response time under specific experimental conditions.

The fluorescence signal of the sensor is a product of the fluorescence of one sensor molecule and the concentration of sensor molecules in a cell. Sensor expression level can vary several-fold between cells, so it is important to normalize the signal by sensor concentration in order to compare measurements between different cells. Several approaches can be used for normalization. First, FRET sensors have two fluorescence proteins, and the FRET signal intensity can be divided by the intensity of a donor fluorescence protein to produce a normalized readout. Second, several sensors (e.g., Peredox) are engineered to have a second

fluorescence protein that does not respond to changes in the sensed molecule and, therefore, the signal from the second fluorescence protein can be used for normalization. Third, fluorescence proteins can be imaged using several excitation wavelengths (e.g., 405nm and 488nm for GFP) and the change in fluorescence in response to binding of the sensed molecule is often different for different wavelength so signal from different excitation wavelengths can be used for normalization. Fourth, treatments that increase the signal above saturation or decrease the signal below the limit of detection can be used for normalization because the signal from a saturated sensor will be entirely driven by its expression level. Table 1 has suggestions for positive control treatments for various sensors that can be used at the end of each experiment to increase the sensed parameter above saturation or decrease below the detection limit of the sensor in each cell. Finally, fluorescence lifetime imaging is independent of sensor concentration but requires advanced lifetime imaging equipment.

Sensors can be calibrated to report the absolute values of the measured parameters. We want to stress that sensor calibration is not a trivial task and care must be taken to avoid introducing systematic errors. Here, we review three approaches for calibration. First, purified sensor protein can be used to make a calibration curve for converting sensor fluorescence into the concentration of metabolites or values of bioenergetic ratios. The data on the dose-response of the purified sensor is often included in the original publication of the sensor. A caveat of the latter approach is that sensor response might vary *in vitro* vs *in vivo* due to differences between intracellular milieu and buffer conditions for *in vitro* measurements. It is important to use an appropriate equation to fit the binding data that accurately accounts for the potential cooperativity of the sensor and minimal/maximal intensity of the sensor[24]. Second, cells expressing the fluorescence sensor can be permeabilized using digitonin or one of the cytolysin pore-forming proteins (e.g., Alpha-toxin (~1–2 nm pore) from Staphylococcus aureus[25], or perfringolysin O (~25 nm pore) from Clostridium perfringens[26]) and calibration curve can be generated by incubating permeabilized cells with a range of concentrations of the sensed metabolite. Third, an orthogonal method can be used to measure the sensed parameter under the same experimental conditions as the sensor, but this is often not feasible as orthogonal methods for measuring compartment-specific values of metabolic parameters do not exist in most cases.

The fluorescence signal is sensitive to pH, ionic strength, and other buffer components. Control experiments should be performed to ensure that a change in signal that is observed during the experiment is not due to a change in pH, ionic strength, photobleaching or other changes unrelated to the parameter of interest. Simple control for the above is to perform experiments in parallel using the full-length sensor and fluorescence protein without the sensor domain. If no change in signal from fluorescence protein is observed, then the experimenter can be more confident that the change in sensor signal is due to the change in the sensed parameter.

## Genetically encoded tools for manipulating metabolism

To establish a causal relationship between a metabolic change and a phenotype, we need novel reagents to directly manipulate metabolite levels and bioenergetic ratios in live cells.

Here, we review the reagents for direct manipulation of metabolism that leverage enzymes for manipulation of metabolite levels or bioenergetic ratios in a spatial and temporal manner (Figure 3). We propose to collectively refer to these reagents as GEMMs – **G**enetically **E**ncoded Tools for **M**anipulation of **M**etabolism. A good example of the promise of this approach for studying metabolism can be found in the field of neuroscience, where optogenetic tools are now widely used to demonstrate causal connections between neuronal activity and physiological outcomes. Similar to GEMMs, optogenetic reagents are a set of genetically encoded tools, which leverage light-sensitive ion channels to directly manipulate plasma membrane potential. We want to highlight that we specifically refer to GEMMs as enzymes that directly manipulate the level of a specific metabolite or a specific bioenergetic ratio and, therefore, can be used to study the function of that specific metabolite or that specific bioenergetic ratio. We do not include master regulators like transcription factors, kinases, or hormone receptors in this category despite their important roles as metabolism regulators. The latter work through indirect mechanisms by manipulating the activities of many enzymes and cannot be used to manipulate the levels of only one metabolite or only one bioenergetic ratio.

The key idea behind GEMMs is to leverage enzymes for the manipulation of metabolite levels or bioenergetic ratios in a spatial and temporal manner. In principle, an ideal GEMM candidate should catalyze a reaction that will change a metabolite level or a bioenergetic ratio of interest and not affect anything else inside the cell. A good GEMM candidate should i) catalyze a reaction that is thermodynamically favorable in living cells, ii) have a sufficiently high catalytic activity (i.e., have low $K_m$ and high $k_{cat}$) to induce manipulation of the desired metabolite or bioenergetic ratio, iii) catalyze reactions that involve either only metabolite(s) of interest or abundant intracellular molecules like water and oxygen to minimize the chance of changing the levels of other metabolites, and iv) be a soluble protein to allow targeting to different subcellular compartments for compartment-specific manipulation of metabolism.

Several GEMMs have been developed to date (Figure 3, Table 2). These includes tools for manipulation of NADH/$NAD^+$ ratio (*Lb*NOX[27]), NADPH/$NADP^+$ ratio (TPNOX[28]), lactate/pyruvate ratio (LOXCAT[29]), $CoQH_2$/CoQ ratio (AOX[30]), $\Delta\Psi_m$ (MitoChR2[31], ABCB-ChR2[32], mtOFF, mtON[33] and mito-dR[34]), superoxide (Killer Red[35,36]), singlet oxygen (miniSOG[37]), and $H_2O_2$ levels (DAAO[38]). Using these GEMMs, researchers can test whether a particular phenotype is caused by changes in these parameters (Figure 4). For example, if Manipulation A leads to a decrease in NADH/$NAD^+$ ratio and leads to phosphorylation of Protein X then *Lb*NOX can be used to induce a decrease in NADH/$NAD^+$ ratio without Manipulation A, and phosphorylation of Protein X can be checked. If *Lb*NOX causes phosphorylation of Protein X then it supports the hypothesis that a decrease in NADH/$NAD^+$ ratio as a result of Manipulation A causes phosphorylation of Protein X. Conversely, GEMMs can be used to rule out a particular parameter from playing a causal role. Table 2 contains key characteristics of available GEMMs including chemical reactions they catalyze, $K_m$, and $k_{cat}$ values. We hope that this information will be useful for researchers as they choose the most relevant GEMM for their experiments.

In addition to GEMMs, there are genetically encoded tools that can be used to bypass endogenous enzymes. NDI1[39] can be used to bypass mitochondrial Complex I. NDI1 is a single polypeptide that catalyzes the same chemical reaction as Complex I but does not pump protons outside of the mitochondrial matrix. NDI1 and its homologs are the alternative forms of mitochondrial Complex I in several fungi and NDI1 is the only form of Complex I in *S. cerevisiae*. Similarly, AOX[40] catalyzes the combined reaction of Complexes III and IV without pumping protons and mito*Lb*NOX expressed in mitochondria catalyzes the combined reaction of the entire mitochondrial electron transport chain (i.e. Complex I, III and IV) without pumping protons. These bypass enzymes are useful to study the causal relationship of proton pumping vs redox homeostasis of ETC enzymes and can be used to rescue phenotypes caused by mutated/inactivated ETC complexes.

Several strategies were used to design and develop GEMMs. The most common approach is to use naturally occurring enzymes. In this approach, biochemical properties especially $K_m$ and $k_{cat}$ value are important to select promising GEMM candidates. *Lb*NOX, AOX, DAAO and NDI1 have been developed using this common approach. MitoChR2, ABCB-ChR2, mtOFF, mtON and mito-dR have been developed using a similar approach where enzymes previously used to manipulate plasma membrane potential to mimic neuronal action potentials where targeted to mitochondria to manipulate $\Delta\Psi_m$. TPNOX, miniSOG and LOXCAT were rationally engineered. In case of TPNOX, a quintuple mutant of *Lb*NOX was developed based on the structure of *Escherichia coli* glutathione reductase (EcGR)-NADPH because there was no naturally occurring $H_2O$-forming oxidases that are highly specific for NADPH. miniSOG were engineered from LOV2 domain of Arabidopsis thaliana phototropin 2 (AtPhot2) using a combination of rational and random mutagenesis to achieve maximal singlet oxygen ($^1O_2$) production[37]. LOXCAT was engineering by fusing a naturally occurring enzyme that convert lactate to pyruvate with another naturally occurring enzyme to detoxify $H_2O_2$ by-product of the first reaction. Finally, KillerRed was identified using a screen for phototoxic homologues of GFP in *E. coli*[35].

GEMMs have already been used in several studies. Direct manipulation of NADH/$NAD^+$ ratio using *Lb*NOX demonstrated that $NAD^+$ recycling, not ATP synthesis, is an essential function of mitochondrial electron transport chain that is required for mammalian cell proliferation[27]. In addition, *Lb*NOX was used in mice to demonstrated that hepatic NADH/$NAD^+$ regulates circulating triglyceride levels, glucose tolerance and FGF21 levels[41]. TPNOX was used to show that NADH/$NAD^+$ and NADPH/$NADP^+$ reduction potentials are connected in the mitochondria but not in the cytosol[28]. Several studies have used NDI and AOX to investigate the requirement of complex I and III of mitochondrial ETC for tumour growth, endothelial cell proliferation and regulatory T cell function *in vivo*[42–45]. All these studies highlight the utility of GEMM to empower studies of ‘causal metabolism’.

## Guidelines for using GEMMs

In this section, we will focus on the aspects of experimental design that should be considered when performing experiments with GEMMs. Controls must be used to ensure that GEMM expression level is sufficient, GEMM is localized to the relevant subcellular compartment, and GEMM reaction by-products do not contribute to observed phenotypes.

We recommend using an inducible expression system for performing experiments with GEMMs. Inducible expression provides several advantages. First, short-term vs long-term effects of metabolic parameter manipulation using GEMM can be studied using inducible expression while only long-term effects will be observed with constitutive expression. Inducible expression of GEMMs is especially important for the application of GEMMs in live animals where it might be useful to induce GEMM expression only in adults to bypass potential developmental effects. Second, the inducible expression of GEMMs allows for rigorously controlled experiments where uninduced cell line or strain can be used as a control. The latter will alleviate a concern that genetic modifications other than GEMM expression introduced during cell line or strain preparation contributed to the phenotype. A catalytically dead mutant of GEMM (or another protein like GFP or Luciferase) can be used as a negative control to verify that the observed effects are due to GEMM catalytic activity and not the effects of inducer or proteotoxic stress. And third, the inducible expression of GEMMs can be used to perform experiments under conditions when a prolonged constitutive expression is toxic to cells or organisms. For mammalian cells and animals, the doxycycline-inducible system allows for inducible expression of GEMMs with minimal leaky expression[46]. Doxycycline is an inhibitor of the mitochondrial ribosome at about ten times higher concentrations than required for maximal inducible expression, so its concentration has to be titrated carefully[47]. In addition, adenovirus and adeno-associated virus vectors can be used for the inducible expression of GEMMs *in vivo*.

GEMMs can be used to manipulate compartment- and tissue-specific metabolic parameters. For compartment-specific manipulation, GEMMs can be targeted to specific organelles by attaching the relevant targeting sequence including mitochondrial targeting sequence, nuclear localization sequence, nuclear exclusion sequence, peroxisomal targeting sequence among others. Similarly, GEMM expression can be induced only in specific tissues using tissue-specific promoters.

It is important to confirm that the parameter of interest is manipulated when GEMMs are expressed. GEMMs are enzymes so their ability to manipulate a metabolic parameter is dependent on expression level. At low levels, GEMMs might not be able to manipulate metabolism significantly so simply confirming that a GEMM is expressed is not sufficient. We anticipate that the ability of GEMMs to manipulate metabolic parameters will be affected by cell types and physiological conditions, so it is important to confirm that GEMM expression manipulates the metabolic parameter in a particular experimental system. In addition, the expression of GEMMs at different levels can be used to observe physiological responses to different levels of manipulation of a metabolic parameter. Several approaches can be used to measure the effect of a GEMM on a metabolic parameter including fluorescence sensors, LC-MS or biochemical assays. Fluorescence sensors reviewed above should be the method of choice when GEMMs are used to manipulate metabolic parameters in subcellular compartments.

In addition to manipulating target metabolic parameters, several GEMMs consume oxygen and produce heat. For example, *Lb*NOX, TPNOX and AOX consume oxygen in addition to manipulating NADH/$NAD^+$, NADPH/$NADP^+$ and $CoQH_2$/CoQ. Most cells can sense and respond to change in oxygen concentration, so it is important to rule out the

effect of oxygen. This can be done by confirming that GEMMs do not affect oxygen concentration using HIF1alpha stability, HIF1alpha target gene expression, or by measuring oxygen concentration using oxygen-sensitive dye or electrode. If GEMMs do lower oxygen concentration, then control experiments should be performed to test whether a decrease in oxygen concentration can induce the phenotype of interest. GEMMs catalyze exergonic reactions that produce heat. GEMMs are unlikely to change the temperature of cells in culture because cells dissipate heat efficiently due to their large surface-to-volume ratio but GEMMs could in theory affect temperature regulation in larger vertebrate animals (i.e., mice) so this must be considered while interpreting the results. One approach for controlling for potential thermoregulation effects of GEMMs expression in large vertebrates would be to perform experiments in thermoneutral conditions.

## Next generation tools for studying metabolism

There are a lot of opportunities to develop new and improved reagents for manipulating and measuring metabolites and bioenergetic ratios. We envision that future work in this area will pursue four broad directions: i) combined use of GEMMs and sensors to study metabolism, ii) design of novel tools for metabolites and bioenergetic ratios that currently cannot be measured or manipulated, iii) improvement of existing tools, and iv) development of novel synthetic biology approaches for tissue- and compartment-specific expression of these tools with precise temporal and expression level control. We believe that these reagents will revolutionize our ability to measure and manipulate metabolism, which will be essential for discovering the molecular mechanisms driving the effect of metabolism on a variety of phenotypes like lifespan and age-associated diseases (Figure 4).

Only a fraction of key metabolites and bioenergetic ratios can be measured or manipulated using available fluorescence sensors and GEMMs (Tables 1, 2). Fluorescence sensors and/or GEMMs for the following key metabolic parameters are awaiting to be developed: many amino acids (major regulators of biosynthesis and cell growth), oxygen (major regulator of energy metabolism), superoxide (key reactive oxygen species), mitochondrial membrane potential (major regulator of mitochondrial physiology), Acetyl-CoA/CoA ratio (major regulator of acetylation and TCA cycle), Fructose-2,6-bisphosphate (major regulator of glycolysis and gluconeogenesis), malonyl-CoA/CoA (major regulator of fatty acid synthesis and oxidation), SAM/SAH (major regulator of methylation). The availability of GEMMs and sensors for these and other key parameters will transform our ability to study compartment- and tissue-specific metabolism.

Most of the key properties of available metabolic sensors can be improved based on the comparison to $Ca^{2+}$ sensors that have gone through several generations of optimization. $Ca^{2+}$ sensors like GCaMPs can now detect physiologically relevant nM concentration of $Ca^{2+}$ and have an impressive dynamic range of fluorescence response of 20–40-fold[48,49]. For comparison, metabolic sensors have a dynamic range of 2–5-fold, are available in only one color, and are responsive to only a small range of a sensed parameter. Based on this comparison, there is room for improvement of current metabolic sensors. Several iterations of $Ca^{2+}$ sensors through mutagenesis can serve as a good roadmap for approaches to improve current metabolic sensors[50]. An important future direction would be to modify

the available sensors to use additional fluorescence proteins with the goal of achieving simultaneous measurement of multiple metabolites. For example, changes in ATP/ADP and NADH/$NAD^+$ ratios can be measured simultaneously if we had compatible fluorescence sensors. Already some of the metabolic sensors (e.g. PercevalHR[51], SoNar[22], HyPer[52] and Citron1[53]) were significantly improved compared to their original version and we hope that other groups will join this exciting field to further improve these and other sensors.

Available GEMMs can be improved in several ways. First, GEMMs with lower $K_m$ and higher $k_{cat}$ can be developed to simplify the application of GEMMs as available GEMMs often have to be expressed at high levels to perturb the target metabolic parameter. The latter can be achieved by rational mutagenesis, directed evolution or by testing additional homologues from evolutionary diverse organisms. Second, catalytically dead versions of GEMMs can be developed for the use as negative controls in GEMM experiments. Third, GEMMs for manipulation of $\Delta\Psi_m$ and superoxide currently require light activation that allows very rapid manipulation of $\Delta\Psi_m$ and superoxide but significantly complicates and limits the types of experiments that can be performed. Availability of GEMMs for manipulation of $\Delta\Psi_m$ and superoxide that do not require light activation will simplify manipulation of $\Delta\Psi_m$ and superoxide. Finally, small molecule inhibitors and activators of GEMMs can be developed to allow for acute activation and inhibition of GEMM activity.

Another important area for improvement of fluorescence sensors and GEMMs is synthetic biology. Application of GEMMs depends on our ability to express GEMMs at different levels, in different tissues and with precise temporal control. GEMMs will benefit from improvement in our ability to quantitatively predict the effect of codon optimization, introns, 5’- and 3’-UTR and Kozak sequences on levels of gene expression. Similarly, further development of inducible expression systems will allow for precise control of level of GEMM expression with temporal resolution. The long-term goal would be to have GEMM constructs that could achieve tuneable GEMM expression with a dynamic range of 10–100-fold and with precise temporal control.

We hope that this overview of available genetically encoded tools for measuring and manipulating metabolism will encourage more people to use these reagents and to join the effort of developing new tools in this area. These genetically encoded tools will empower the research community to answer entirely new questions about the regulation of metabolism and help us uncover the molecular mechanisms that drive the effect of nutrition on aging and age-associated diseases.

## Acknowledgments:

D.V.T. is supported by the NIH Director’s New Innovator Award (DP2-GM132933).

## References:

1. Mair W & Dillin A Aging and Survival: The Genetics of Life Span Extension by Dietary Restriction. Annu. Rev. Biochem 77, 727–754 (2008). [PubMed: 18373439]
2. Warburg O, Wind F & Negelein E THE METABOLISM OF TUMORS IN THE BODY. J. Gen. Physiol 8, 519–530 (1927). [PubMed: 19872213]

3. DeBerardinis RJ & Chandel NS We need to talk about the Warburg effect. Nat. Metab 2, 127–129 (2020). [PubMed: 32694689]
4. Fontana L, Meyer TE, Klein S & Holloszy JO Long-term calorie restriction is highly effective in reducing the risk for atherosclerosis in humans. Proc. Natl. Acad. Sci. U. S. A 101, 6659–6663 (2004). [PubMed: 15096581]
5. Lean ME et al. Primary care-led weight management for remission of type 2 diabetes (DiRECT): an open-label, cluster-randomised trial. The Lancet 391, 541–551 (2018).
6. Wen CP et al. Minimum amount of physical activity for reduced mortality and extended life expectancy: a prospective cohort study. Lancet Lond. Engl 378, 1244–1253 (2011).
7. Aune D et al. Fruit and vegetable intake and the risk of cardiovascular disease, total cancer and all-cause mortality-a systematic review and dose-response meta-analysis of prospective studies. Int. J. Epidemiol 46, 1029–1056 (2017). [PubMed: 28338764]
8. Blangy D, Buc H & Monod J Kinetics of the allosteric interactions of phosphofructokinase from Escherichia coli. J. Mol. Biol 31, 13–35 (1968). [PubMed: 4229913]
9. Pettit FH, Pelley JW & Reed LJ Regulation of pyruvate dehydrogenase kinase and phosphatase by acetyl-CoA/CoA and NADH/NAD ratios. Biochem. Biophys. Res. Commun 65, 575–582 (1975). [PubMed: 167775]
10. Carling D, Clarke PR, Zammit VA & Hardie DG Purification and characterization of the AMP-activated protein kinase. Copurification of acetyl-CoA carboxylase kinase and 3-hydroxy-3-methylglutaryl-CoA reductase kinase activities. Eur. J. Biochem 186, 129–136 (1989). [PubMed: 2598924]
11. Zhang Q, Piston DW & Goodman RH Regulation of corepressor function by nuclear NADH. Science 295, 1895–1897 (2002). [PubMed: 11847309]
12. Dunne MJ & Petersen OH Intracellular ADP activates K+ channels that are inhibited by ATP in an insulin-secreting cell line. FEBS Lett. 208, 59–62 (1986). [PubMed: 2429868]
13. Gibson D & Harris RA Metabolic Regulation in Mammals. (CRC Press, 2001).
14. Lin VS, Dickinson BC & Chang CJ Boronate-based fluorescent probes: imaging hydrogen peroxide in living systems. Methods Enzymol. 526, 19–43 (2013). [PubMed: 23791092]
15. Su Y & Hammond MC RNA-based fluorescent biosensors for live cell imaging of small molecules and RNAs. Curr. Opin. Biotechnol 63, 157–166 (2020). [PubMed: 32086101]
16. Mannan AA, Liu D, Zhang F & Oyarzún DA Fundamental Design Principles for Transcription-Factor-Based Metabolite Biosensors. ACS Synth. Biol 6, 1851–1859 (2017). [PubMed: 28763198]
17. Greenwald EC, Mehta S & Zhang J Genetically Encoded Fluorescent Biosensors Illuminate the Spatiotemporal Regulation of Signaling Networks. Chem. Rev 118, 11707–11794 (2018). [PubMed: 30550275]
18. Gutscher M et al. Real-time imaging of the intracellular glutathione redox potential. Nat. Methods 5, 553–559 (2008). [PubMed: 18469822] This article introduces GPX1-roGFP1 as a fluorescence sensor for measuring GSSG/GSH ratio.
19. Gutscher M et al. Proximity-based Protein Thiol Oxidation by $H_2O_2$-scavenging Peroxidases. J. Biol. Chem 284, 31532–31540 (2009). [PubMed: 19755417] This article introduces Orp1-roGFP1 as a fluorescence sensor for measuring $H_2O_2$ levels.
20. Morgan B et al. Real-time monitoring of basal H 2 O 2 levels with peroxiredoxin-based probes. Nat. Chem. Biol 12, 437–443 (2016). [PubMed: 27089028]
21. Tao R et al. Genetically encoded fluorescent sensors reveal dynamic regulation of NADPH metabolism. Nat. Methods 14, 720–728 (2017). [PubMed: 28581494]
22. Zhao Y et al. SoNar, a Highly Responsive NAD+/NADH Sensor, Allows High-Throughput Metabolic Screening of Anti-tumor Agents. Cell Metab. 21, 777–789 (2015). [PubMed: 25955212] This article introduces SoNar as a fluorescence sensor for measuring NADH/$NAD^+$ ratio.
23. Sanderson MJ, Smith I, Parker I & Bootman MD Fluorescence Microscopy. Cold Spring Harb. Protoc 2014, pdb.top071795 (2014). [PubMed: 25275114]
24. Pomorski A, Kochańczyk T, Miłoch A & Krężel A Method for Accurate Determination of Dissociation Constants of Optical Ratiometric Systems: Chemical Probes, Genetically Encoded Sensors, and Interacting Molecules. Anal. Chem 85, 11479–11486 (2013). [PubMed: 24180305]

25. Bhakdi S et al. Staphylococcal alpha-toxin, streptolysin-O, and Escherichia coli hemolysin: prototypes of pore-forming bacterial cytolysins. Arch. Microbiol 165, 73–79 (1996). [PubMed: 8593102]
26. Shepard LA et al. Identification of a membrane-spanning domain of the thiol-activated pore-forming toxin Clostridium perfringens perfringolysin O: an alpha-helical to beta-sheet transition identified by fluorescence spectroscopy. Biochemistry 37, 14563–14574 (1998). [PubMed: 9772185]
27. Titov DV et al. Complementation of mitochondrial electron transport chain by manipulation of the NAD+/NADH ratio. Science 352, 231–235 (2016). [PubMed: 27124460] This article reports the use of LbNOX as a tool for manipulation of NADH/$NAD^+$ ratio. Authors use LbNOX to demonstrate that NAD+ recycling, not ATP synthesis, is an essential function of mitochondrial ETC required for cell proliferation.
28. Cracan V, Titov DV, Shen H, Grabarek Z & Mootha VK A genetically encoded tool for manipulation of NADP+/NADPH in living cells. Nat. Chem. Biol 13, 1088–1095 (2017). [PubMed: 28805804] This article introduces TPNOX as a tool for manipulation of NADPH/$NADP^+$ ratio.
29. Patgiri A et al. An engineered enzyme that targets circulating lactate to alleviate intracellular NADH:NAD+ imbalance. Nat. Biotechnol 38, 309–313 (2020). [PubMed: 31932725]
30. Guarás A et al. The CoQH2/CoQ Ratio Serves as a Sensor of Respiratory Chain Efficiency. Cell Rep. 15, 197–209 (2016). [PubMed: 27052170]
31. Tkatch T et al. Optogenetic control of mitochondrial metabolism and Ca2+ signaling by mitochondria-targeted opsins. Proc. Natl. Acad. Sci. U. S. A 114, E5167–E5176 (2017). [PubMed: 28611221]
32. Graf SA, Haigh SE, Corson ED & Shirihai OS Targeting, Import, and Dimerization of a Mammalian Mitochondrial ATP Binding Cassette (ABC) Transporter, ABCB10 (ABC-me). J. Biol. Chem 279, 42954–42963 (2004). [PubMed: 15215243]
33. Berry BJ et al. Optogenetic control of mitochondrial protonmotive force to impact cellular stress resistance. EMBO Rep. 21, e49113 (2020). [PubMed: 32043300]
34. Imai Y et al. Light-driven activation of mitochondrial proton-motive force improves motor behaviors in a Drosophila model of Parkinson's disease. Commun. Biol 2, 424 (2019). [PubMed: 31799427]
35. Bulina ME et al. A genetically encoded photosensitizer. Nat. Biotechnol 24, 95–99 (2006). [PubMed: 16369538] This article introduces KillerRed as a photosensitizer and superoxide producer.
36. Pletnev S et al. Structural Basis for Phototoxicity of the Genetically Encoded Photosensitizer KillerRed *. J. Biol. Chem 284, 32028–32039 (2009). [PubMed: 19737938]
37. Shu X et al. A Genetically Encoded Tag for Correlated Light and Electron Microscopy of Intact Cells, Tissues, and Organisms. PLoS Biol. 9, e1001041 (2011). [PubMed: 21483721] This article describes the development of miniSOG.
38. Haskew-Layton RE et al. Controlled enzymatic production of astrocytic hydrogen peroxide protects neurons from oxidative stress via an Nrf2-independent pathway. Proc. Natl. Acad. Sci 107, 17385–17390 (2010). [PubMed: 20855618]
39. Seo BB, Wang J, Flotte TR, Yagi T & Matsuno-Yagi A Use of the NADH-quinone oxidoreductase (NDI1) gene of Saccharomyces cerevisiae as a possible cure for complex I defects in human cells. J. Biol. Chem 275, 37774–37778 (2000). [PubMed: 10982813]
40. Kido Y et al. Purification and kinetic characterization of recombinant alternative oxidase from Trypanosoma brucei brucei. Biochim. Biophys. Acta BBA - Bioenerg. 1797, 443–450 (2010).
41. Goodman RP et al. Hepatic NADH reductive stress underlies common variation in metabolic traits. Nature 583, 122–126 (2020). [PubMed: 32461692]
42. McElroy GS et al. NAD+ Regeneration Rescues Lifespan, but Not Ataxia, in a Mouse Model of Brain Mitochondrial Complex I Dysfunction. Cell Metab. 32, 301–308.e6 (2020). [PubMed: 32574562]
43. Martínez-Reyes I et al. Mitochondrial ubiquinol oxidation is necessary for tumour growth. Nature 585, 288–292 (2020). [PubMed: 32641834]

44. Weinberg SE et al. Mitochondrial complex III is essential for suppressive function of regulatory T cells. Nature 565, 495–499 (2019). [PubMed: 30626970]
45. Diebold LP et al. Mitochondrial complex III is necessary for endothelial cell proliferation during angiogenesis. Nat. Metab 1, 158–171 (2019). [PubMed: 31106291]
46. Das AT, Tenenbaum L & Berkhout B Tet-On Systems For Doxycycline-inducible Gene Expression. Curr. Gene Ther 16, 156–167 (2016). [PubMed: 27216914]
47. Moullan N et al. Tetracyclines Disturb Mitochondrial Function across Eukaryotic Models: A Call for Caution in Biomedical Research. Cell Rep. 10, 1681–1691 (2015). [PubMed: 25772356]
48. Lin MZ & Schnitzer MJ Genetically encoded indicators of neuronal activity. Nat. Neurosci 19, 1142–1153 (2016). [PubMed: 27571193]
49. Shen Y, Nasu Y, Shkolnikov I, Kim A & Campbell RE Engineering genetically encoded fluorescent indicators for imaging of neuronal activity: Progress and prospects. Neurosci. Res 152, 3–14 (2020). [PubMed: 31991206]
50. Zhao Y et al. An Expanded Palette of Genetically Encoded Ca2+ Indicators. Science 333, 1888–1891 (2011). [PubMed: 21903779]
51. Tantama M, Martínez-François JR, Mongeon R & Yellen G Imaging energy status in live cells with a fluorescent biosensor of the intracellular ATP-to-ADP ratio. Nat. Commun 4, 2550 (2013). [PubMed: 24096541] This article introduces PercevalHR as a fluorescence sensor for measuring ATP/ADP ratio.
52. Bilan DS et al. HyPer-3: A Genetically Encoded H2O2 Probe with Improved Performance for Ratiometric and Fluorescence Lifetime Imaging. ACS Chem. Biol 8, 535–542 (2013). [PubMed: 23256573]
53. Zhao Y, Shen Y, Wen Y & Campbell RE High-Performance Intensiometric Direct- and Inverse-Response Genetically Encoded Biosensors for Citrate. ACS Cent. Sci 6, 1441–1450 (2020). [PubMed: 32875085]
54. Park JO et al. Metabolite concentrations, fluxes and free energies imply efficient enzyme usage. Nat. Chem. Biol 12, 482–489 (2016). [PubMed: 27159581]
55. Chen WW, Freinkman E, Wang T, Birsoy K & Sabatini DM Absolute Quantification of Matrix Metabolites Reveals the Dynamics of Mitochondrial Metabolism. Cell 166, 1324–1337.e11 (2016). [PubMed: 27565352]
56. Hung YP, Albeck JG, Tantama M & Yellen G Imaging Cytosolic NADH-NAD+ Redox State with a Genetically Encoded Fluorescent Biosensor. Cell Metab. 14, 545–554 (2011). [PubMed: 21982714]
57. Krebs HA The redox state of nicotinamide adenine dinucleotide in the cytoplasm and mitochondria of rat liver. Adv. Enzyme Regul 5, 409–434 (1967). [PubMed: 4301794]
58. Cambronne XA et al. Biosensor reveals multiple sources for mitochondrial NAD+. Science 352, 1474–1477 (2016). [PubMed: 27313049]
59. Zou Y et al. Illuminating NAD+ Metabolism in Live Cells and In Vivo Using a Genetically Encoded Fluorescent Sensor. Dev. Cell 53, 240–252.e7 (2020). [PubMed: 32197067]
60. Sallin O et al. Semisynthetic biosensors for mapping cellular concentrations of nicotinamide adenine dinucleotides. eLife 7, e32638 (2018). [PubMed: 29809136]
61. Lu W, Wang L, Chen L, Hui S & Rabinowitz JD Extraction and Quantitation of Nicotinamide Adenine Dinucleotide Redox Cofactors. Antioxid. Redox Signal 28, 167–179 (2018). [PubMed: 28497978]
62. Zhu X-H, Lu M, Lee B-Y, Ugurbil K & Chen W In vivo NAD assay reveals the intracellular NAD contents and redox state in healthy human brain and their age dependences. Proc. Natl. Acad. Sci 112, 2876–2881 (2015). [PubMed: 25730862]
63. Yu Q & Heikal AA Two-photon autofluorescence dynamics imaging reveals sensitivity of intracellular NADH concentration and conformation to cell physiology at the single-cell level. J. Photochem. Photobiol. B 95, 46–57 (2009). [PubMed: 19179090]
64. Gribble FM et al. A Novel Method for Measurement of Submembrane ATP Concentration. J. Biol. Chem 275, 30046–30049 (2000). [PubMed: 10866996]

65. Dragon S, Hille R, Götz R & Baumann R Adenosine 3′:5′-Cyclic Monophosphate (cAMP)-Inducible Pyrimidine 5′-Nucleotidase and Pyrimidine Nucleotide Metabolism of Chick Embryonic Erythrocytes. Blood 91, 3052–3058 (1998). [PubMed: 9531619]
66. Imamura H et al. Visualization of ATP levels inside single living cells with fluorescence resonance energy transfer-based genetically encoded indicators. Proc. Natl. Acad. Sci 106, 15651–15656 (2009). [PubMed: 19720993]
67. Yaginuma H et al. Diversity in ATP concentrations in a single bacterial cell population revealed by quantitative single-cell imaging. Sci. Rep 4, 6522 (2014). [PubMed: 25283467]
68. Lobas MA et al. A genetically encoded single-wavelength sensor for imaging cytosolic and cell surface ATP. Nat. Commun 10, 711 (2019). [PubMed: 30755613]
69. Gu H et al. A novel analytical method for in vivo phosphate tracking. FEBS Lett. 580, 5885–5893 (2006). [PubMed: 17034793]
70. van Eunen K et al. Measuring enzyme activities under standardized in vivo-like conditions for systems biology: Standardized enzyme assays for systems biology. FEBS J. 277, 749–760 (2010). [PubMed: 20067525]
71. Tao R et al. Genetically encoded fluorescent sensors reveal dynamic regulation of NADPH metabolism. Nat. Methods 14, 720–728 (2017). [PubMed: 28581494]
72. Veech RL, Eggleston LV & Krebs HA The redox state of free nicotinamide–adenine dinucleotide phosphate in the cytoplasm of rat liver. Biochem. J 115, 609–619 (1969). [PubMed: 4391039]
73. Shaik IH & Mehvar R Rapid determination of reduced and oxidized glutathione levels using a new thiol-masking reagent and the enzymatic recycling method: application to the rat liver and bile samples. Anal. Bioanal. Chem 385, 105–113 (2006). [PubMed: 16547740]
74. Montero D, Tachibana C, Rahr Winther J & Appenzeller-Herzog C Intracellular glutathione pools are heterogeneously concentrated. Redox Biol. 1, 508–513 (2013). [PubMed: 24251119]
75. Pak VV et al. Ultrasensitive Genetically Encoded Indicator for Hydrogen Peroxide Identifies Roles for the Oxidant in Cell Migration and Mitochondrial Function. Cell Metab. 31, 642–653.e6 (2020). [PubMed: 32130885]
76. Sies H Hydrogen peroxide as a central redox signaling molecule in physiological oxidative stress: Oxidative eustress. Redox Biol. 11, 613–619 (2017). [PubMed: 28110218]
77. Stone JR & Yang S Hydrogen Peroxide: A Signaling Messenger. Antioxid. Redox Signal. 8, 243–270 (2006). [PubMed: 16677071]
78. Takanaga H, Chaudhuri B & Frommer WB GLUT1 and GLUT9 as major contributors to glucose influx in HepG2 cells identified by a high sensitivity intramolecular FRET glucose sensor. Biochim. Biophys. Acta BBA - Biomembr. 1778, 1091–1099 (2008).
79. Hu H et al. Glucose monitoring in living cells with single fluorescent protein-based sensors. RSC Adv. 8, 2485–2489 (2018).
80. Arce-Molina R et al. A highly responsive pyruvate sensor reveals pathway-regulatory role of the mitochondrial pyruvate carrier MPC. eLife 9, e53917 (2020). [PubMed: 32142409]
81. Bulusu V et al. Spatiotemporal Analysis of a Glycolytic Activity Gradient Linked to Mouse Embryo Mesoderm Development. Dev. Cell 40, 331–341.e4 (2017). [PubMed: 28245920]
82. San Martín A et al. A Genetically Encoded FRET Lactate Sensor and Its Use To Detect the Warburg Effect in Single Cancer Cells. PLoS ONE 8, e57712 (2013). [PubMed: 23469056]
83. Leippe D, Sobol M, Vidugiris G, Cali JJ & Vidugiriene J Bioluminescent Assays for Glucose and Glutamine Metabolism: High-Throughput Screening for Changes in Extracellular and Intracellular Metabolites. SLAS Discov. Adv. Sci. Drug Discov 22, 366–377 (2017).
84. Lønbro S et al. Reliability of blood lactate as a measure of exercise intensity in different strains of mice during forced treadmill running. PLOS ONE 14, e0215584 (2019). [PubMed: 31050686]
85. Zhang C, Wei Z-H & Ye B-C Quantitative monitoring of 2-oxoglutarate in Escherichia coli cells by a fluorescence resonance energy transfer-based biosensor. Appl. Microbiol. Biotechnol 97, 8307–8316 (2013). [PubMed: 23893310]
86. Wang W et al. A Ratiometric Fluorescent Biosensor Reveals Dynamic Regulation of Long-Chain Fatty Acyl-CoA Esters Metabolism. Angew. Chem. Int. Ed 60, 13996–14004 (2021).

87. Faergeman NJ & Knudsen J Role of long-chain fatty acyl-CoA esters in the regulation of metabolism and in cell signalling. Biochem. J 323 (Pt 1), 1–12 (1997). [PubMed: 9173866]

88. Gruenwald K et al. Visualization of Glutamine Transporter Activities in Living Cells Using Genetically Encoded Glutamine Sensors. PLOS ONE 7, e38591 (2012). [PubMed: 22723868]

89. Marvin JS et al. An optimized fluorescent probe for visualizing glutamate neurotransmission. Nat. Methods 10, 162–170 (2013). [PubMed: 23314171]

90. Hires SA, Zhu Y & Tsien RY Optical measurement of synaptic glutamate spillover and reuptake by linker optimized glutamate-sensitive fluorescent reporters. Proc. Natl. Acad. Sci 105, 4411–4416 (2008). [PubMed: 18332427]

91. Hu H et al. A genetically encoded toolkit for tracking live-cell histidine dynamics in space and time. Sci. Rep 7, 43479 (2017). [PubMed: 28252043]

92. Okada S, Ota K & Ito T Circular permutation of ligand-binding module improves dynamic range of genetically encoded FRET-based nanosensor. Protein Sci 18, 2518–2527 (2009). [PubMed: 19827096]

93. Yoshida T, Nakajima H, Takahashi S, Kakizuka A & Imamura H OLIVe: A Genetically Encoded Fluorescent Biosensor for Quantitative Imaging of Branched-Chain Amino Acid Levels inside Single Living Cells. ACS Sens. 4, 3333–3342 (2019). [PubMed: 31845569]

94. Liu X et al. PPM1K Regulates Hematopoiesis and Leukemogenesis through CDC20-Mediated Ubiquitination of MEIS1 and p21. Cell Rep. 23, 1461–1475 (2018). [PubMed: 29719258]

95. Zhang WH et al. Monitoring hippocampal glycine with the computationally designed optical sensor GlyFS. Nat. Chem. Biol 14, 861–869 (2018). [PubMed: 30061718]

96. Kaper T et al. Nanosensor Detection of an Immunoregulatory Tryptophan Influx/Kynurenine Efflux Cycle. PLOS Biol. 5, e257 (2007). [PubMed: 17896864]

97. Zhu A, Romero R & Petty HR A sensitive fluorimetric assay for pyruvate. Anal. Biochem 396, 146–151 (2010). [PubMed: 19748474]

98. Liu X et al. Acetate Production from Glucose and Coupling to Mitochondrial Metabolism in Mammals. Cell 175, 502–513.e13 (2018). [PubMed: 30245009]

99. Rosini E, Caldinelli L & Piubelli L Assays of D-Amino Acid Oxidase Activity. Front. Mol. Biosci 4, 102 (2017). [PubMed: 29404340]

100. Velázquez I & Pardo JP Kinetic Characterization of the Rotenone-Insensitive Internal NADH: Ubiquinone Oxidoreductase of Mitochondria from Saccharomyces cerevisiae. Arch. Biochem. Biophys 389, 7–14 (2001). [PubMed: 11370674]

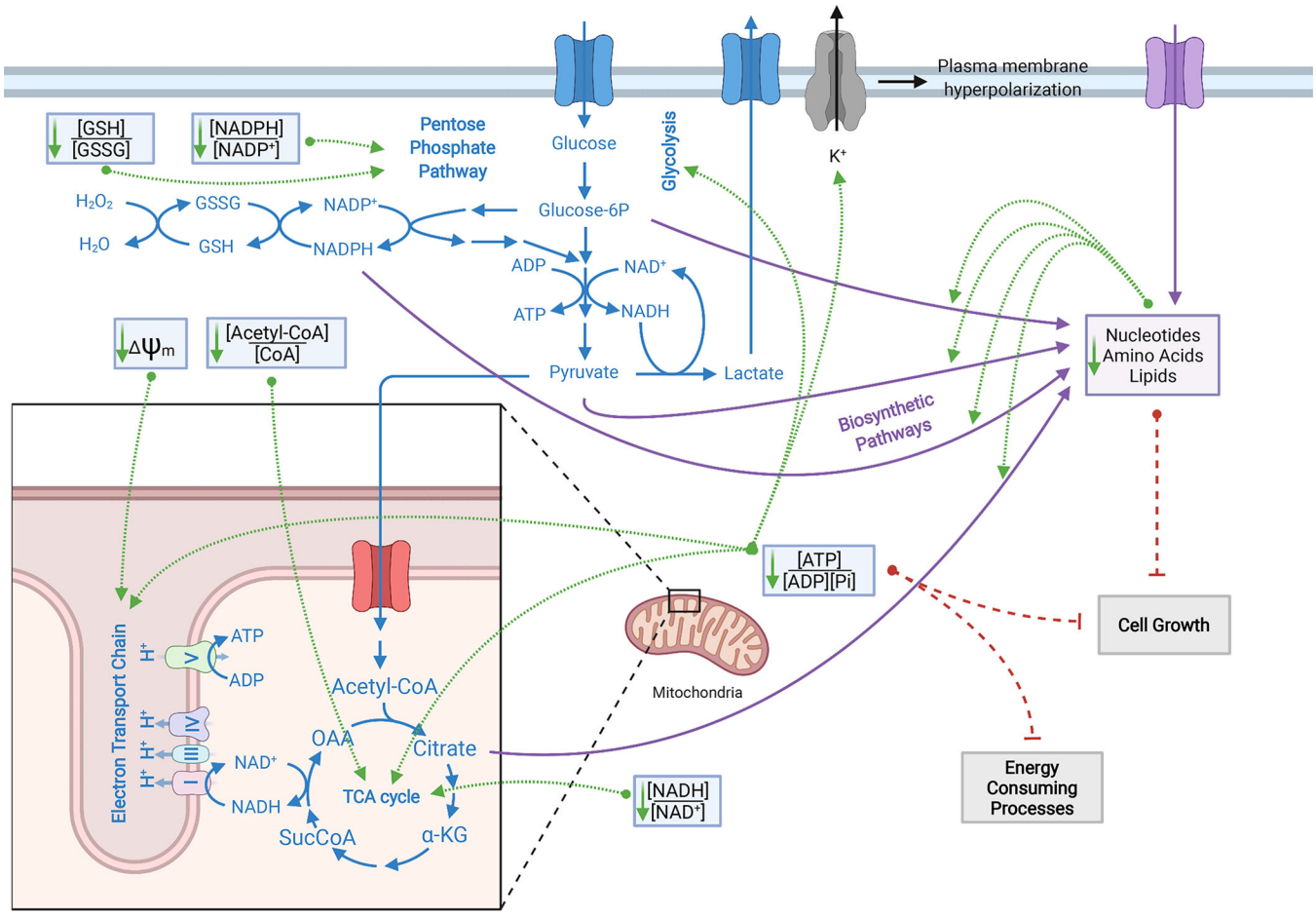


**Figure 1.**

Overview of the regulation of metabolism and cell physiology by nucleotides, amino acids, lipids, and bioenergetic ratios.

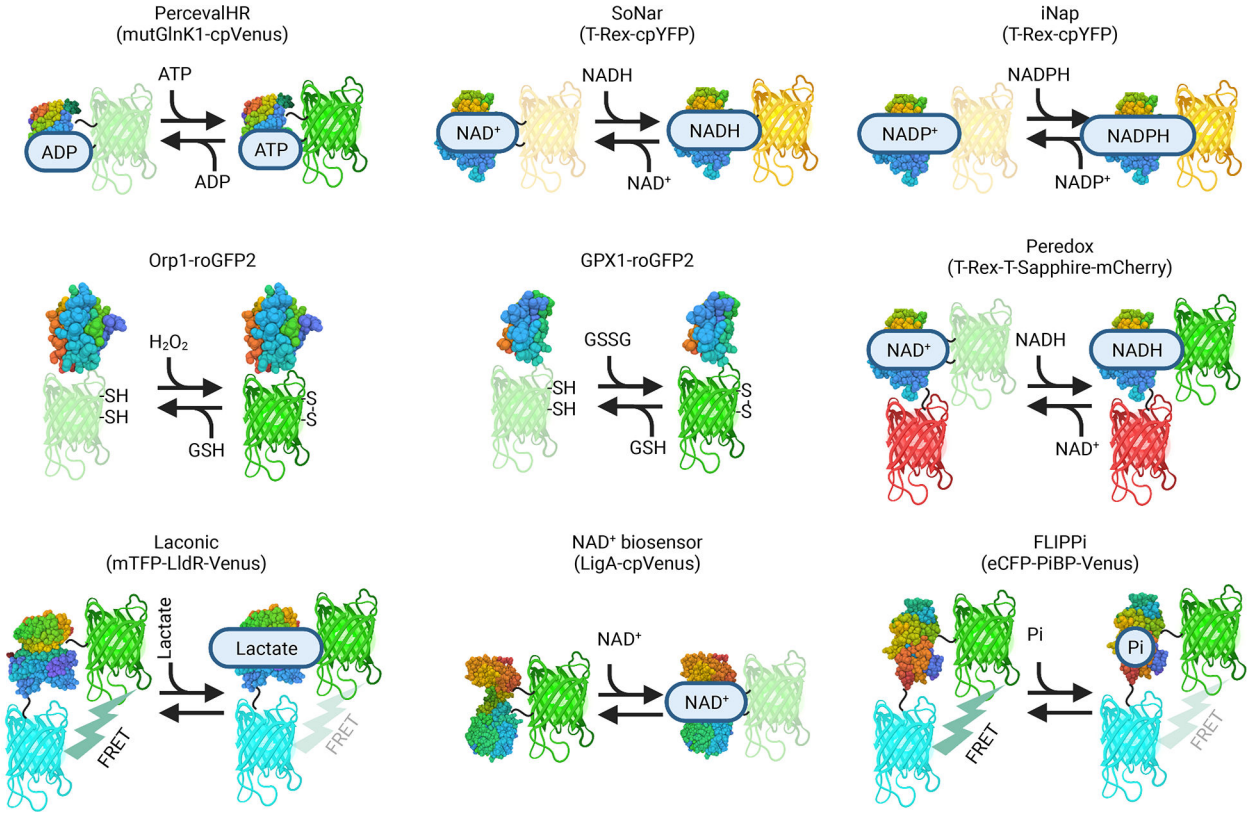


**Figure 2.**

Schematic structures of select fluorescence sensor for measuring metabolism. The binding of a metabolite causes a conformational change that results in a change in fluorescence properties of the sensor like brightness or FRET. Depicted structures of sensors are made by merging the structures of sensing domains and fluorescence proteins and do not represent actual structures of full-length sensors, which have not been determined. The following PDB structures of sensing domains were used: LigA (5TT5), PiBP(1A40), LldR(2DI3), T-Rex (1XCB), Orp1 (3CMI), Gpx1 (7C10), GlnK1 (2J9E).

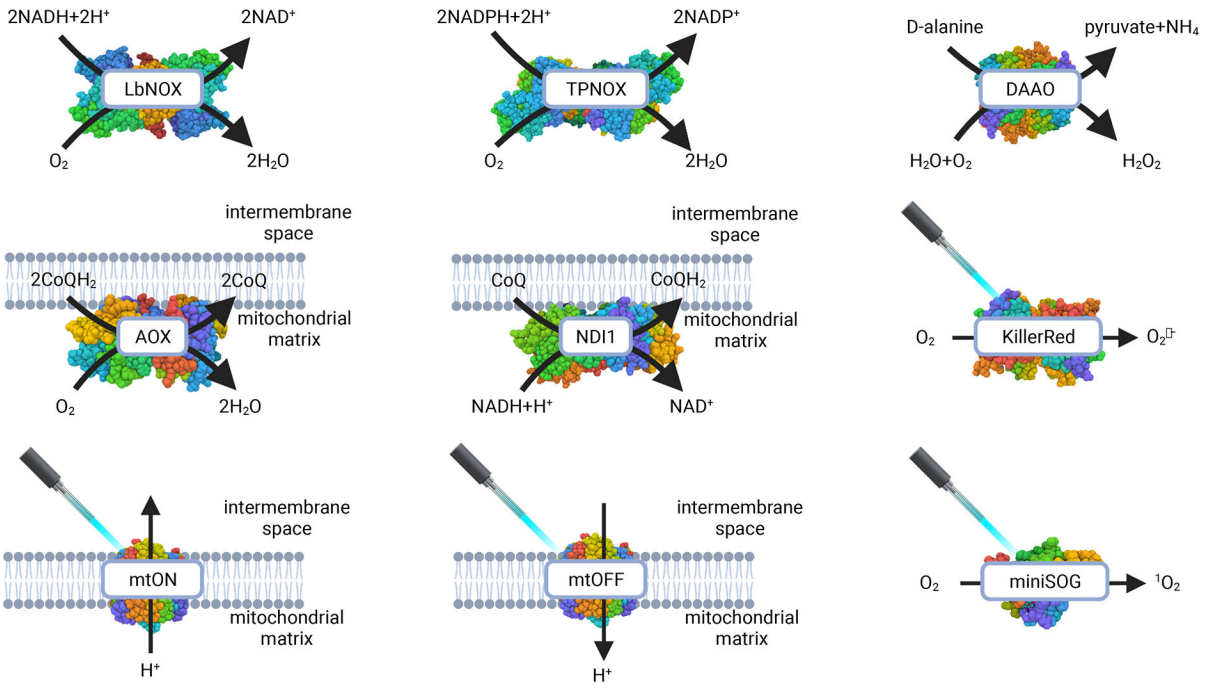


**Figure 3.**

Structures and reactions catalyzed by several available GEMMs. Light activation is required for activation of mtOFF, for driving proton pumping of mtON against proton-motive force and for production of superoxide by KillerRed and singlet oxygen by miniSOG. The following PDB structures were used: LbNOX (5ER0), TPNOX(5VOH), AOX(3VV9), NDI1(4G9K), DAAO(1C0I), mtON(1QKO), mtOFF(1QKO), KillerRed (3GB3) and miniSOG(6GPU).

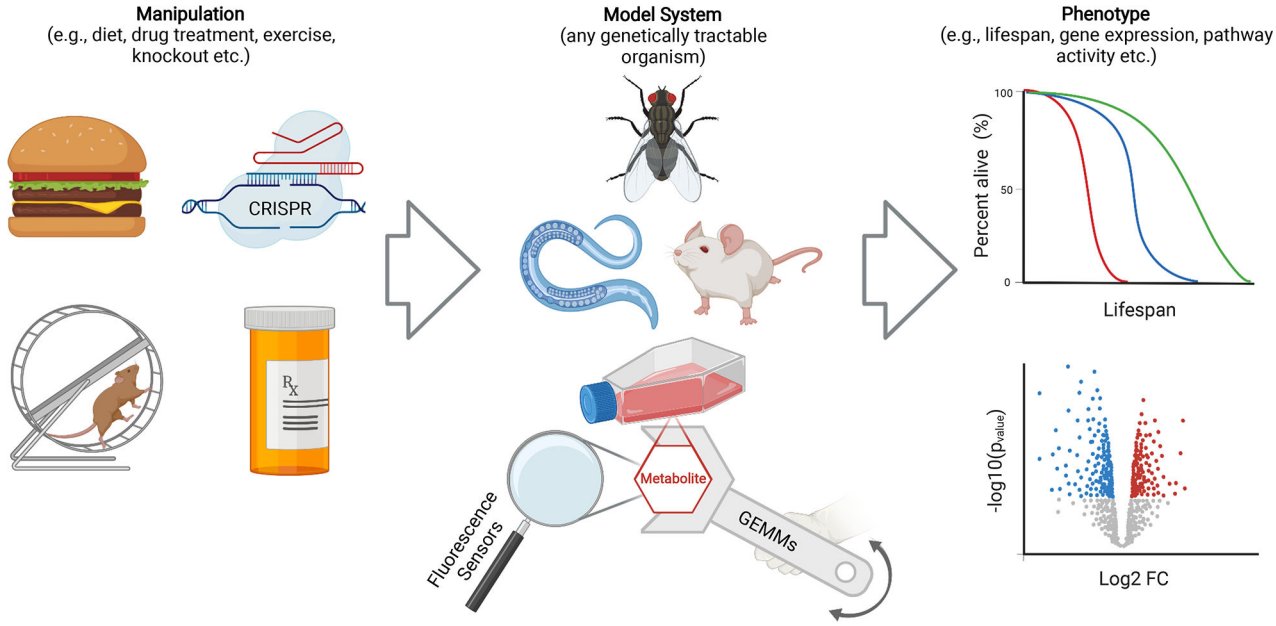


**Figure 4.**

Schematic of the use of GEMMs and fluorescence sensors. GEMMs can be used to mimic the effect of treatments on specific metabolites and bioenergetic ratios. The latter can be used to establish the causal role of a metabolic parameter changes in mediating the effect of treatment on the phenotype of interest. Fluorescence sensors can be used to measure metabolites and bioenergetic ratio in live cells and organisms.

**Table 1.**

Properties of genetically encoded sensors.

| Sensed Parameter | Name of Sensor | $EC_{50}$ | Detectable range of parameter | Dynamic range ($\Delta F/F_{min}$) | Physiological range of parameter[54,55] | Positive control |
|---|---|---|---|---|---|---|
| Bioenergetic parameters | | | | | | |
| **NADH/NAD$^+$** | **Peredox**[56]<br>**SoNar**[22]<br>Frex | 0.01<br>0.025 | 0.001–0.05<br>0.001–1 | 1.5<br>15 | Cytosolic: 0.05–0.01[57]<br>Mitochondrial: 0.1–0.2[57] | Antimycin A<br>FCCP |
| **NAD$^+$** | **NAD$^+$ biosensor** [58]<br>**FiNad** [59]<br>**NAD-Snifit** [60] | 60μM<br>1.3mM<br>60μM | 0.01–1 mM<br>0.1–10mM<br>0.01–1mM | 2<br>7<br>7 | 0.1–0.4mM[61–63] | Nicotinamide riboside<br>FK866 |
| **ATP/ADP** | **PercevalHR** [51] | 3.5 | 0.4–40 | 3 | 1–50[54,55,64,65] | Oligomycin<br>Glucose withdrawal |
| **ATP** | **Ateam** [66]<br>**QUEEN** [67]<br>**iATPSnFR** [68] | 3mM<br>2mM<br>150μM | 1–10mM<br>1–10mM<br>10μM-1mM | 1.5<br>3<br>2.4 | 1–10mM[64,65] | Oligomycin<br>Glucose withdrawal |
| **Phosphate** | **FLIPPi** [69] | 1μM-30mM | 0.1μM-100mM | 0.5–0.7 | 1–10mM[70] | Phosphate |
| **NADPH** | **iNap** [21] | 1–20μM | 0.1–1000μM | 8 | 10–200μM[61,71] | $H_2O_2$, diamide |
| **NADPH/ NADP$^+$** | **NADP-Snifit** [60] | 30 | 1–100 | 7 | 10–100[72] | $H_2O_2$ diamide |
| **GSH/GSSG** | **GRX1-roGFP2** [18] | 40 | 5–100 GSH/GSSG | 8 | 10–100[73,74] | $H_2O_2$ diamide |
| **$H_2O_2$** | **Orp1-roGFP2** [19]<br>**HyPer** [75] | 0.5μM<br>0.1μM | 0.05–10μM ($H_2O_2$)<br>0.01–1μM ($H_2O_2$) | 6<br>4 | 1–700 nM[76,77] | $H_2O_2$ diamide |
| Intermediary metabolism | | | | | | |
| **Glucose** | **FLII$^{12}$Pglu-700μδ6** [78] | 0.7mM<br>0.03–3mM | 0.05–10mM<br>1μM-100mM | 0.7<br>5 | 3–10 mM (human blood) | Glucose |

| Sensed Parameter | Name of Sensor | $EC_{50}$ | Detectable range of parameter | Dynamic range ($\Delta F/F_{min}$) | Physiological range of parameter[54,55] | Positive control |
|---|---|---|---|---|---|---|
| | **FGBP** [79] | | | | | |
| **Pyruvate** | **PyronicSF** [80]<br>**PYRATES** [81] | 0.5 mM<br>65 μM | 0.03–3mM<br>0.01–1mM | 2.5<br>0.2 | ~300μM[55] | Pyruvate |
| **Lactate** | **Laconic** [82] | 0.1mM | 1μM-10mM | 0.2 | 1–10mM[83,84] | Lactate |
| **Citrate** | **Citron1** [53]<br>**Citroff1** [53] | 1.1mM<br>5 μM | 0.01–10mM<br>1–100μM | 9<br>18 | 0.5–1mM[54,55] | Glucose<br>BMS-303141<br>Antimycin A |
| **α-ketoglutarate** | **OGsor** [85] | 0.7mM | 0.1–10mM | −0.75 | ~1mM[54,55] | Glutamine |
| **Long Chain Fatty Acyl-CoA** | **LACSer** [86] | 0.3–0.7μM | 0.01–100μM | 1.2 | 1–200nM[87] | Long chain fatty acids |
| Amino acids | | | | | | |
| **Glutamine** | **FLIPQ-TV3.0** [88] | 1μM-8mM | 0.1μM-20mM | 0.1–0.26 | 1–20mM[54,55] | Glutamine |
| **Glutamate** | **iGluSnFR** [89]<br>**GluSnFR** [90] | 110μM<br>2μM | 1μM - 1mM<br>0.1–10μM | 4.5<br>0.44 | 20–60mM[54,55] | Glutamate |
| **Histidine** | **FHisJ** [91]<br>**FLIP-cpHisJ194** [92] | 22μM<br>14μM | 1μM - 1mM<br>1μM - 1mM | 5<br>0.63 | 0.5–1mM[54,55] | Histidine |
| **BCAA** | **OLIVe** [93]<br>**BCAA sensor** [94] | 0.1–1mM<br>1–10μM | 0.01–10mM<br>0.1–100μM | 0.9<br>1.6 | 3–5mM[54,55] | BCAA |
| **Glycine** | **GlyFS** [95] | 20μM | 1μM-1mM | 0.2 | 3–6mM[54,55] | Glycine |
| **Arginine** | **FLIP-cpArtJ185** [92] | 10μM | 1–100μM | 0.5 | 0.1–0.3mM[54,55] | Arginine |

| **Sensed Parameter** | **Name of Sensor** | **$EC_{50}$** | **Detectable range of parameter** | **Dynamic range ($\Delta F/F_{min}$)** | **Physiological range of parameter[54,55]** | **Positive control** |
|---|---|---|---|---|---|---|
| **Tryptophan** | **FLIPW** [96] | 100μM | 15μM-1mM | 0.3 | ~0.2mM[54,55] | Tryptophan |

*Values are rounded to two significant digits and one significant digit for physiological range.

**Table 2.**

Chemical reactions catalyzed by GEMMs and their kinetic parameters.

| GEMM | Chemical reaction | $K_m$ (μM) | $k_{cat}$ ($s^{-1}$) | Physiological concentration of metabolites |
|---|---|---|---|---|
| **LbNOX** [27] | $2NADH + 2H^+ + O_2 \rightarrow 2NAD^+ + 2H_2O$ | 70 (NADH) | 650 | 1–200 μM (NADH)[61–63]<br>100–400 μM ($NAD^{+3}$)[61–63] |
| **TPNOX** [28] | $2NADPH + 2H^+ + O_2 \rightarrow 2NADP^+ + 2H_2O$ | 24 (NADPH) | 310 | 3–200 μM (NADPH)[21,61]<br>5–70 μM ($NADP^+$)[21,61] |
| **LOXCAT** [29] | $2Lactate + 2H^+ + O_2 \rightarrow 2Pyruvate + 2H_2O$ | 570 (Lactate) | 340 | 1–10 mM (Lactate)[83,84]<br>200–400 uM (Pyruvate)[97,98] |
| **DAAO** [99] | $D\text{-alanine} + H_2O + O_2 \rightarrow pyruvate + NH_4^+ + H_2O_2$ | 1.0 (Alanine) | 80 | 1–700 nM ($H_2O_2$)[76,77] |
| **NDM** [100] | $NADH + H^+ + CoQ \rightarrow NAD^+ + CoQH_2$ | 9.4 (NADH) | 80 | 1–200 uM (NADH)[61–63]<br>~100–400 uM ($NAD^+$)[61–63] |
| **AOX** [40] | $2CoQH_2 + O_2 \rightarrow 2CoQ + 2H_2O$ | 340 ($CoQH_2$) | 410 | ND |
| **MitoChR2** [31]<br>**ABCB-ChR2** [32]<br>**mtOFF** | $H^+_{\text{mito matrix}} + h\gamma \rightarrow H^+_{\text{mito intermembrane space}}$ | ND | ND | $\Delta\Psi_m$ ~ 150–220mV |
| **mtON** [33]<br>**mito-dR** [34] | $H^+_{\text{mito intermembrane space}} + h\gamma \rightarrow H^+_{\text{mito matrix}}$ | ND | ND | pH ~7.4 cyto<br>pH ~ 7.8 mito<br>$\Delta\Psi_m$ ~ 150–220mV |
| **miniSOG** [37] | $O_2 + h\gamma \rightarrow {}^1O_2$ (singlet oxygen) | ND | ND | << 1pM |
| **Killer Red** [35] | $O_2 + h\gamma \rightarrow O_2^{\bullet-}$(superoxide) | ND | ND | 1–100pM |

*Values are rounded to two significant digits and one significant digit for physiological range.